

# Thermoreversible gelation of syndiotactic polystyrene in toluene and chloroform\*

Christophe Daniel, Alain Menelle†, Annie Brulett and Jean-Michel Guenet‡

Laboratoire D'Ultrasons et de Dynamique des Fluides Complexes, Université Louis Pasteur-CNRS URA 851, 4, rue Blaise Pascal, F-67070 Strasbourg Cedex, France and †Laboratoire Léon Brillouin, CEA-CNRS, CEN Saclay, 91191 Gif-Sur-Yvette Cedex, France  
 (Revised 8 November 1996)

Temperature–concentration phase diagrams have been established for syndiotactic polystyrene (sPS)/toluene gels and sPS/chloroform gels. The occurrence of polymer–solvent compound formation is shown in both systems and confirmed by neutron diffraction investigations. In particular it is found that a compound with a stoichiometry close to 1/1 occurs in both types of gels. Infra-red analysis show that the polymer chains take on a  $2_1$  helical form in both series of gels. In sPS/toluene gels, neutron scattering experiments reveal that the chains possess a worm-like conformation in the molten state while still retaining a conformation close to the  $2_1$  helix. The results are discussed in the light of a polymer–solvent intercalation model already proposed for sPS/benzene gels. © 1997 Elsevier Science Ltd.

(Keywords: syndiotactic polystyrene; thermoreversible gels; phase diagrams; molecular structure)

## INTRODUCTION

The interactions between a polymer and a solvent have been and still are extensively studied, especially when crystallizable polymers are dealt with, as is the case for highly syndiotactic polystyrene (sPS). This polymer, which was first synthesized only a few years ago<sup>1,2</sup>, has been the subject of many studies<sup>3–7</sup> that have revealed a very complex polymorphic behaviour. Through different thermal or solvent processings sPS can crystallize under two different crystalline lattices wherein the chain conformation takes on a transplanar zigzag arrangement ( $T_4$ ). These two crystalline forms are usually designated as  $\alpha$  and  $\beta$  in the literature. The sPS chains can also adopt a  $2_1$  helix conformation ( $T_2G_2$ ) through solvent-induced crystallization of glassy amorphous samples<sup>3</sup> or through solvent exposure of the  $\alpha$  form<sup>2</sup>. The new form, usually designated as  $\delta$ , leads to the formation of a polymer–solvent compound<sup>8</sup>.

Further, like isotactic polystyrene (iPS) and atactic polystyrene (aPS), sPS can also form thermoreversible gels in many solvents<sup>9–11</sup>. Since sPS can display helical structures that differ significantly from that of iPS, new possibilities are offered for understanding the gelation phenomenon, and particularly for testing the cavity model<sup>12,13</sup>. This model considers that solvent molecules are housed within the cavities formed by adjacent phenyl groups of the  $3_1$  helix, which results in helix stabilization and eventually prevents the chains from folding. The only remaining possibility for the chains

to organize is then to create a fibrillar morphology as is expected for a gel.

The purpose of this paper is to report on studies of the thermal behaviour of sPS/toluene and sPS/chloroform systems in order to find out to which extent the solvent is involved in thermoreversible gelation of sPS. The gel molecular structure will be then investigated by neutron scattering, neutron diffraction and Fourier transform infra-red (FTi.r.) spectroscopy.

## EXPERIMENTAL

### Materials

All sPS samples, hydrogenous (sPSH) and deuterated (sPSD), were synthesized following the method devised by Grassi *et al.*<sup>2</sup>. The <sup>1</sup>H nuclear magnetic resonance characterization showed that the content of syndiotactic triads was over 99%. The different molecular weights were determined by gel permeation chromatography in dichlorobenzene at 140°C:

$$\text{sPSD1 } M_w = 4.3 \times 10^4 \text{ with } M_w/M_n = 3.6$$

$$\text{sPSD2 } M_w = 1.5 \times 10^5 \text{ with } M_w/M_n = 2.4$$

$$\text{sPSH1 } M_w = 1.0 \times 10^5 \text{ with } M_w/M_n = 4.4$$

$$\text{sPSH2 } M_w = 4.9 \times 10^5 \text{ with } M_w/M_n = 4.3$$

Benzene and chloroform, either protonated or deuterated (over 99% deuterated) were purchased from Aldrich and used without further purification.

### Techniques and sample preparation

*Differential scanning calorimetry (d.s.c.).* The gel thermal behaviour was investigated by means of a DSC 30 apparatus from Mettler. For concentrations below

\* This work has been supported by a grant from the EEC (Human Capital and Mobility Programme) enabling the creation of a laboratories network entitled: 'Polymer–Solvent Organization in Relation to Chain Microstructure'

‡ To whom correspondence should be addressed

30% (w/w) in toluene or in chloroform, homogeneous solutions were prepared in test-tubes and a gel was formed. A piece of the gel was then introduced into stainless steel pans that were hermetically sealed with a special device. We checked that solvent loss was minimum while transferring from the test-tube to the sample pan. For higher concentrations, pieces of gel were prepared by solvent evaporation.

Prior to any measurements the gels were melted in the d.s.c. pan and quenched at room temperature for toluene and at  $T = 0^\circ\text{C}$  for chloroform in order to reform the gels. A heating rate of  $5^\circ\text{C m}^{-1}$  was used for all the samples.

**Neutron diffraction.** Neutron diffraction experiments were carried out on G-6-1, a diffraction camera located at Orphée (Laboratoire Léon Brillouin). G-6-1 is a two-axis spectrometer equipped with a banana-type  $\text{BF}_3$  detector composed of 400 cells with an angular resolution of  $0.2^\circ$ . The spectrometer operates at a wavelength  $\lambda = 0.474\text{ nm}$  obtained by diffraction of the neutron beam on to a graphite monocrystal oriented under Bragg conditions (further details available on request). By rotation of the detector the following  $q$  range was made accessible:

$$2\text{ nm} < q < 25\text{ nm}^{-1} \text{ with } q = (4\pi/\lambda)\sin(\theta/2)$$

Detector normalization was achieved with a vanadium sample.

The samples were prepared in quartz tubes of 4 mm inner diameter. The desired quantities of polymer (sample sPSD1) and solvent were introduced together. The cell was sealed hermetically from the atmosphere and heated well above the solvent's boiling temperature so as to obtain a homogeneous solution. Gels were obtained by a rapid quench to room temperature for toluene and to  $T = 0^\circ\text{C}$  for chloroform.

**I.r. spectroscopy.** I.r. spectra were obtained by using a Nicolet 60SX FTi.r. spectrometer equipped with a multichannel detector possessing a  $2\text{ cm}^{-1}$  resolution; 32 scans were performed per spectrum. The samples were first prepared in hermetically sealed test-tubes, and then were rapidly transferred on to KBr plates, squeezed and scanned. The whole operation took approximately less than 3 min, which allowed minimum solvent evaporation.

**Small-angle neutron scattering.** Small-angle neutron scattering studies, restricted to sPS/toluene systems, were performed on the PACE camera located at Orphée (Laboratoire Léon Brillouin, Saclay, France). On this camera the neutron detector consists of concentric rings regularly spaced so that a ring of radius  $r$  corresponds to a scattering vector  $q = 4\pi/\lambda\sin(\theta/2)$  with  $\theta = \arctan(r/D)$ , where  $D$  = sample-detector distance. This detector can be moved to different distances from the sample. A mechanical selector provides neutrons with a wavelength distribution characterized by a relative full width at half-maximum,  $\Delta\lambda/\lambda_m$ , of about 10%. By using different sample-detector distances and  $\lambda_m = 0.6\text{ nm}$ , the available  $q$  range was:

$$0.1 \leq q \leq 2.5\text{ nm}^{-1}$$

Samples were prepared in hermetically sealed

rectangular quartz cells into which the desired quantity of each constituent was introduced beforehand. The mixture was heated until a clear, homogeneous solution was obtained. The gels were produced by a rapid quench to room temperature.

The gels consisted of a few per cent of deuterated chains imbedded in the gel matrix. This matrix was composed of protonated polymer together with a mixture of deuterated solvent and protonated solvent, the composition of which was calculated in such a way as to match the scattering amplitude of the protonated polymer (10.2% toluene-*D*/89.8% toluene-*H*, v/v). Under these conditions a blank sample free of deuterated chains showed a virtually flat scattering of incoherent nature in the whole  $q$  range. This incoherent signal was subtracted after the usual transmissions and thickness corrections from the intensity scattered by the deuterium-labelled samples so as to extract the coherent intensity arising from the deuterated chains.

The position sensitive counter was calibrated by using a solvent of purely incoherent scattering (*cis*-decalin in the present case). Under these conditions the absolute intensity,  $I_A(q)$  is written:

$$I_A = I_N(q)/K \quad (1)$$

in which  $I_N(q)$  is the intensity obtained after background subtraction, transmission corrections and detector normalization, and  $K$  is a constant which includes the contrast factor and is written:

$$K = \frac{4\pi \times \delta \times N_A \times T_{\text{dec}} \times (a_H - a_D)^2}{g(\lambda) \times m_0^2 \times (1 - T_{\text{dec}})} \quad (2)$$

in which  $N_A$  is the Avogadro number,  $m_0$  is the monomer molecular weight,  $T_{\text{dec}}$  and  $\delta$  are the *cis*-decalin sample transmission and thickness, respectively,  $a_D$  and  $a_H$  are the scattering amplitudes of the deuterated polymer and of the protonated polymer, respectively, and  $g(\lambda)$  is a corrective term which depends upon the neutron wavelength, the wavelength distribution and the camera. This parameter was determined here by means of a method devised by Cotton<sup>14</sup>.

## RESULTS AND DISCUSSION

Solutions from sPS in chloroform usually produce only a gel independent of the cooling rate. The gelation kinetics is relatively slow unless the solutions are quenched at very low temperatures. Conversely, depending upon the cooling rate, the two types of morphologies can be obtained with toluene: *fibrillar* gels or *spherulitic packing*. Fibrillar gels, which are the systems of interest according to the definition of thermoreversible gels given in a previous paper<sup>10</sup>, are obtained by a rapid quench. It is worth underlining that only the morphology is altered by the preparation procedure but not the thermal behaviour.

### *Thermal behaviour: temperature-concentration phase diagram*

For a sheer question of availability, the d.s.c. investigations in toluene were carried out with the sPSD2 sample and in chloroform with sPSH2.

**Phase behaviour in toluene.** Typical d.s.c. traces are given in *Figure 1* for different polymer concentrations.

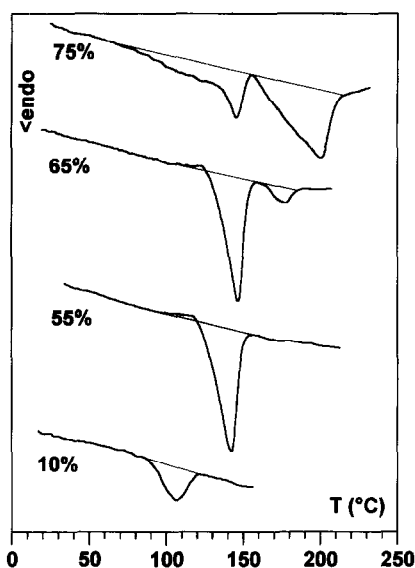


Figure 1 Typical d.s.c. traces obtained on heating at  $5^{\circ}\text{Cm}^{-1}$  sPS/toluene gels. Concentrations in w/w as indicated

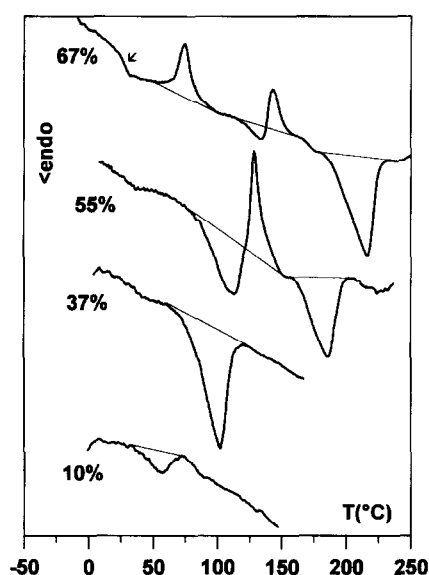


Figure 3 Typical d.s.c. traces obtained on heating at  $5^{\circ}\text{Cm}^{-1}$  sPS/chloroform gels. Arrow indicates the glass transition. Concentrations in w/w as indicated

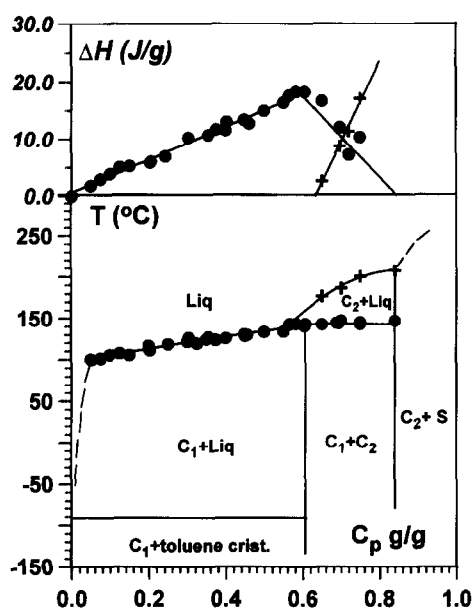


Figure 2 Bottom: temperature-concentration phase diagram for the system sPS/toluene. As is customary, full lines stand for known transitions while dotted lines stand for probable extensions: ● fusion of  $C_1$ ; (+) fusion of  $C_2$ . Top: Tamman's plots: enthalpies associated with the various thermal events: (●) fusion of  $C_1$ ; (+) fusion of  $C_2$

As can be seen the d.s.c. display one melting endotherm up to a concentration  $C_p = 0.65$  (w/w) (low melting endotherm). For more concentrated systems a second melting endotherm (high-melting endotherm) appears at higher temperature.

The temperature associated with the low-melting endotherm increases with increasing concentrations up to  $C_p = 0.56$  (w/w), and then remains nearly constant at larger concentrations ( $T_{\text{low}} = 144 \pm 3^{\circ}\text{C}$  for  $C_p > 0.56$  w/w). The temperature associated with the high-melting endotherm increases continuously with increasing temperature in the range of concentrations investigated.

The temperature-concentration phase diagram drawn in Figure 2 highlights these different types of behaviour. The variations of the enthalpies associated with each endotherm as a function of polymer concentration

(Tamman's plots) are represented in the same figure. The enthalpy associated with the low-melting endotherm first increases linearly up to a polymer concentration  $C_p = 0.6$  and then decreases to become zero at about  $C_p = 0.83$  (w/w). Conversely, the enthalpy associated with the high-melting endotherm increases continuously. The enthalpy variations and the shape of the phase diagram are consistent with the existence of two compounds  $C_1$  and  $C_2$  of differing stoichiometries.  $C_1$  is an *incongruently melting compound* which transforms into  $C_2$  at  $T_{\text{low}}$ . This conclusion is reached because the concentration at which  $T_{\text{low}}$  becomes a constant differs from the concentration at which the associated enthalpy is maximum. The stoichiometry of compound  $C_1$  is given by the latter polymer concentration, namely about 0.8 toluene molecules per monomer unit. The stoichiometry of compound  $C_2$  is given by the concentration for which the enthalpy of the low melting endotherm is zero ( $C_p \approx 0.83$  w/w), namely one toluene molecule per four monomeric units. It is worth noticing that this stoichiometry corresponds to that given by Chatani *et al.*<sup>8</sup> for the compound they obtained by exposure to toluene vapours.

It must be emphasized that if the sample's crystallinity varied when changing the polymer concentration, then straight lines, as is the case here, would not be obtained. Consequently, the stoichiometries deduced from Tamman's plots are the actual values.

Beyond the concentration corresponding to the stoichiometry of compound  $C_2$  no information is presently available as it is quite difficult to prepare highly concentrated homogeneous samples.

*Phase behaviour in chloroform.* As can be seen in Figure 3, the d.s.c. traces for gels prepared from chloroform differ from those obtained with toluene in that recrystallization phenomena are observed beyond  $C_p = 0.4$  (w/w). Up to this concentration the d.s.c. traces display only one low-melting endotherm whose peak temperatures increase with increasing concentration. Above  $C_p = 0.4$  (w/w) the low-melting endotherm is followed by a crystallization exotherm,

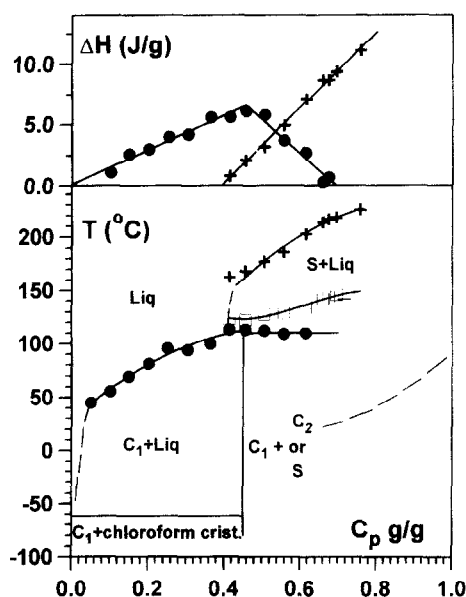


**Figure 4** Bottom: temperature-concentration phase diagram for the system sPS/chloroform. As is customary, full lines stand for known transitions while dotted lines stand for probable extensions: (●) fusion of  $C_1$ ; (+) fusion of S; (◇) glass transition; (□) recrystallization. Top: Tamman's plots: enthalpies associated with the various thermal events: (●) fusion of  $C_1$ ; (+) fusion of S

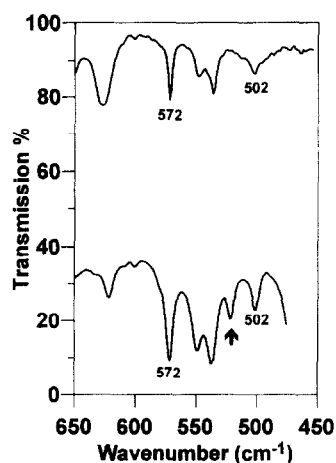


**Figure 5** I.r. spectra. Bottom: sPS/toluene gel ( $C_p = 0.1$  w/w); top: sPS/chloroform gel ( $C_p = 0.02$  w/w)

which is in turn followed by a high-melting endotherm. Furthermore, beyond  $C_p = 0.6$  (w/w), a glass transition followed by a low-temperature crystallization exotherm appears.

The temperature associated with the low melting-endotherm increases with increasing concentration up to about  $C_p = 0.4$  (w/w) and then remains constant ( $T_{\text{low}} = 110 \pm 3^{\circ}\text{C}$ ). Conversely, the temperatures associated with the crystallization exotherm and the high-melting endotherm increase. All the different transitions give the phase diagram drawn in Figure 4. In the same figure are represented the variations of the enthalpies associated with each endotherm as a function of polymer concentration (Tamman's plots). The low-melting endotherm enthalpy first increases linearly up to a maximum occurring at  $C_p \approx 0.44$  (w/w) and then decreases linearly to become zero at  $C_p \approx 0.70$  (w/w). Conversely, the enthalpy of the high-melting endotherm increases continuously. The variations of

the low-melting enthalpies and melting temperatures are consistent with the existence of a compound  $C_1$  given by the maximum of the enthalpy, whose stoichiometry is one chloroform molecule per monomer unit. This compound is also an incongruently melting compound as the maximum in the low-melting endotherm enthalpy and the invariance of  $T_{\text{low}}$  do not occur at the same concentration. At higher concentrations two situations must be contemplated: either there exists a second compound  $C_2$  whose stoichiometry is given by the concentration at which the low-melting enthalpy becomes zero, namely about one chloroform molecule per three monomer units, or the melting of compound  $C_1$  gives a solid solution S. As we have no diffraction information in this range of concentration we cannot conclude on this point. The stoichiometry 1/3 is not, however, in register with the helix symmetry so that a solid solution appears to be a more likely structure. Here, the transformation of compound  $C_1$  is not direct as the system undergoes a fusion-recrystallization as opposed to what is seen in benzene.

In summary, the knowledge of the phase diagrams has revealed the existence of solvated structures both in sPS gels from toluene and from chloroform as was already reported for sPS/benzene gels<sup>11</sup> and iPS/decalin gels<sup>15</sup>. The phase diagrams suggest two different stoichiometries in chloroform (stoichiometry 1/1) and in toluene (stoichiometry 0.8/1). As with benzene, two compounds have also been discovered in toluene although the compounds in sPS/benzene are far more solvated than those here (four benzene molecules per monomer unit and one benzene molecule per monomer unit, respectively). This highlights the fact that slight modifications on the solvent molecule (an additional methyl group on toluene with respect to benzene) has definitely tremendous consequences on the compound structure. Worth emphasizing is the fact that sPS/toluene systems, for which the stoichiometry is lower than 1/1 (0.8/1), is the only system that gives spherulites instead of fibres when low cooling rates are brought about. In chloroform and benzene, spherulites are never produced whatever the cooling rate used. This point will be further discussed below.

#### Molecular structure

*I.r. analysis.* A convenient way to find out what type of helical structure is involved in the gels consists in performing an i.r. spectroscopy study as the absorption spectrum changes dramatically whether the planar zigzag form or the  $2_1$  helix is present. These two forms exhibit differing characteristic i.r. absorption bands<sup>16-18</sup>, as 1349, 1224 and 537  $\text{cm}^{-1}$  for the planar zigzag and at 1354, 1277, 572 and 502  $\text{cm}^{-1}$  for the  $2_1$  helix.

The kind of structure involved in sPS/chloroform gels and the conformational ordering process have already been described in the literature<sup>9,19</sup>. It has been shown that at low concentrations (typically 0.02 w/w), the spectrum of the gel state reveals the presence of the  $2_1$  form, which establishes that the helical form is involved in compound  $C_1$  of sPS/chloroform gels.

The i.r. spectra in the range 450–650  $\text{cm}^{-1}$  for a 0.1 (w/w) sPS/toluene gel and a 0.02 (w/w) sPS chloroform are given in Figure 5. As can be seen the spectra exhibit the same absorption bands (the additional peak at 526  $\text{cm}^{-1}$  is due to toluene). We can conclude that the  $2_1$  form is

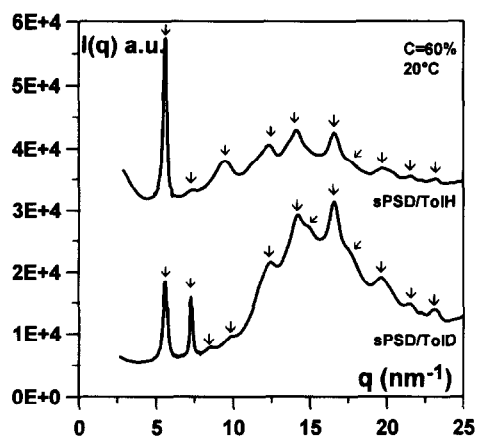


**Figure 6** Neutron diffraction pattern for 60% gels (corresponding to stoichiometry of compound  $C_1$ ). Top: deuterated polystyrene in hydrogenous toluene; bottom: deuterated polystyrene in deuterated toluene

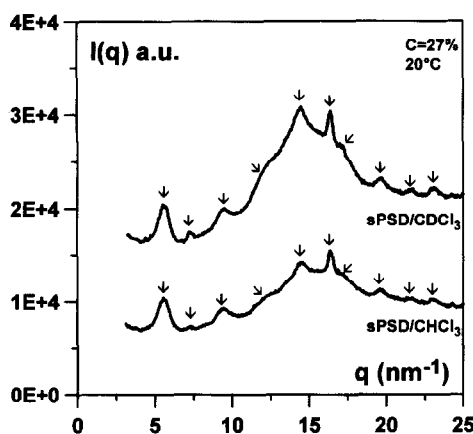


**Figure 7** Neutron diffraction pattern for 0.27 (w/w) gels. Top: deuterated polystyrene in deuterated chloroform; bottom: deuterated polystyrene in hydrogenous chloroform

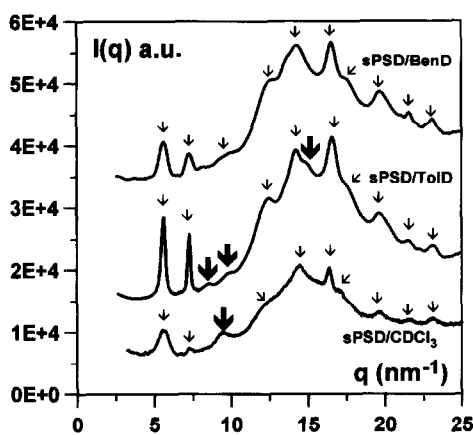


**Figure 8** Neutron diffraction patterns of gels composed from top to bottom: deuterated polystyrene in deuterated benzene ( $C_p = 0.57$  w/w); deuterated polystyrene in deuterated toluene ( $C_p = 0.6$  w/w); deuterated polystyrene in deuterated chloroform ( $C_p = 0.27$  w/w)

also present in both sPS/toluene and sPS/chloroform gels.

**Neutron diffraction.** For determining the chains' mutual organization, diffraction techniques are required. Neutron diffraction is an appropriate tool for studying

polymer-solvent compounds as the labelling of either component provides one with four structure factors without significant alteration of the molecular arrangement. Neutron diffraction together with isotopic labelling gives immediate evidence of the existence of a compound<sup>20</sup>. This is illustrated by examining the theoretical expression for the intensity given by a system containing two types of molecules:

$$I(q) \simeq A_p^2(q)S_p(q) + A_s^2(q)S_s(q) + 2A_p(q)A_s(q)S_{ps}(q) \quad (3)$$

in which  $A(q)$  and  $S(q)$ , with the appropriate subscripts, are the contrast factor and the structure factor of the polymer and the solvent, and  $S_{ps}(q)$  is a cross-term between solvent and polymer. If the system is non-solvated, i.e. absence of any polymer-solvent compound, the cross-term can be discarded provided that the crystal size is large enough. By changing the value of the contrast factor of the polymer, the overall diffracted intensity will change, but the ratios between the diffraction peaks will remain unchanged. Conversely, for polymer-solvent compounds, these ratios will differ due to the cross-term, which cannot be neglected any longer.

Here, results obtained at 20°C at a concentration  $C_p = 0.6$  (w/w) for sPS/toluene gel (Figure 6) and  $C_p = 0.27$  (w/w) for sPS/chloroform gel (Figure 7) are presented and discussed qualitatively. Detailed calculations of the structure factors which take into account the isotopic labelling are in progress and their outcome will be reported in due course.

As can be seen in Figures 6 and 7, the intensities differ when the labelling is altered. For instance, all the samples display a reflection at  $7.2 \text{ nm}^{-1}$  which is stronger for sPSD/toluene-*D* and sPSD/chloroform-*D* than for sPSD/toluene-*H* and sPSD/chloroform-*H*. This clearly supports the existence of a solvated structure with intercalation of the solvent molecules in the crystalline lattice and thus confirms the above results obtained by d.s.c. Furthermore, the diffraction patterns obtained for both solvents, although displaying some discrepancies (indicated by bold arrows in Figure 8), are qualitatively consistent with the crystalline lattice proposed by Chatani *et al.*<sup>8</sup> (monoclinic with  $a = 1.758 \text{ nm}$ ,  $b = 1.326 \text{ nm}$ ,  $c = 0.771 \text{ nm}$  and  $\gamma = 121.2^\circ$ ; space group  $P2_1/a$ ).

However, for the sPS/toluene case, these authors suggest a stoichiometry of 1/4 toluene/monomeric units. While Chatani *et al.*'s lattice seems to be a good starting candidate for the compounds, a finer tuning is needed, with particular emphasis on the placement of the solvent molecules. In what follows, this issue will be discussed from the neutron scattering results, by means of a molecular model.

It is worth noticing that the positions of the reflections peaks are identical for sPS/benzene<sup>11</sup> and sPS/chloroform gels (in both cases the stoichiometry is 1/1).

#### Chain conformation

To determine the chain trajectory in the gel system it is necessary that only the coherent scattering be that of the deuterated chains. The coherent scattering arising from the protonated chains has, therefore, to be matched by using an appropriate mixture of deuterated and

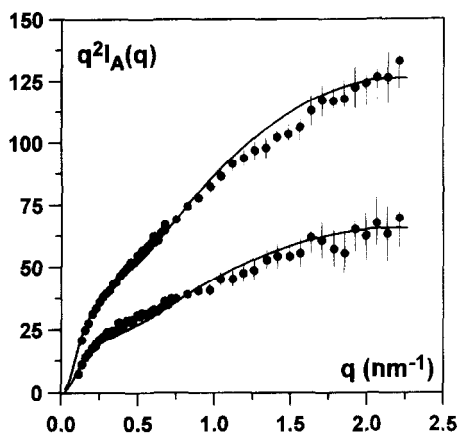


**Figure 9** Neutron scattering curves represented by means of a Kratky plot [ $q^2 I_A(q)$  versus  $q$ ] for sPS/toluene gel ( $C_p = 0.12$  w/w) in the molten state. Data obtained at two sample-detector distances. Top:  $C_D = 0.06$  (w/w); bottom:  $C_D = 0.03$  (w/w). The full lines represent the best fit obtained through the use of Yoshisaki and Yamakawa's relationship<sup>23</sup>

hydrogenated solvents. While this can be achieved with toluene, this matching process is unfortunately impossible with chloroform.

The chain conformation was investigated for sPS/toluene gels in the gel state and in the molten state ( $T = 140^\circ\text{C}$ ) for an overall polymer concentration of 0.12 (w/w), which corresponds to the system being under compound  $C_1$  structure. The overall concentrations of deuterium-labelled sPS were 0.06 and 0.03 (w/w), respectively.

We first discuss the results obtained in the molten state that are shown in *Figure 9* by means of a Kratky representation [ $q^2 I(q)$  versus  $q$ ]. As was already suggested for the same type of results obtained for molten sPS/benzene systems, the scattering curves are reminiscent of that given by a worm-like chain. For an infinitely long and infinitely thin Brownian chain characterized by a persistence length  $l_p$ , there exist two asymptotic regimes on either side of a momentum transfer ( $q^*$ )<sup>21,22</sup>:

$$\begin{aligned} \text{for } q < q^* \quad q^2 I(q) &= 6\mu_L/l_p \\ \text{for } q > q^* \quad q^2 I(q) &= \mu_L[\pi q + 2/l_p] \end{aligned} \quad (4)$$

in which  $\mu_L$  is the mass per unit length.  $q^*$  is then written:

$$q^* = 16/3\pi l_p \approx 1.7/l_p \quad (5)$$

If the chain possesses a non-negligible transverse cross-section as is the case for a helical form such as the  $2_1$  helix, the cross-section effect has to be taken into account in equation (4) for  $q > q^*$ . Provided that the cross-section is smaller than the persistence length and by neglecting the constant term in equation (4), the intensity is written for  $q > q^*$ :

$$q^2 I_A(q) = \pi C_D \mu_L q f(qr_H) \quad (6)$$

In the case of helical form of radius  $r_H$ ,  $f(qr_H)$  is written at low-resolution<sup>23</sup>:

$$f(qr_H) = 4J_1^2(qr_H)/(qr_H)^2 \quad (7)$$

So far, infinitely long chains have been considered. Yoshisaki and Yamakawa<sup>24</sup> have derived a semi-analytical expression for finite chains of contour length

$L$  for  $ql_p < 5$ . Their equations are particularly useful for  $q < q^*$ . For  $q > q^*$ , equation (6) can be used as soon as  $ql_p > 5$ . The following parameters for an ideal worm-like chain have been used for the fits shown in *Figure 9*:

$$L = 72 \text{ nm}, l_p = 9 \text{ nm.}$$

$$r_H = 0.62 \pm 0.1 \text{ nm, and } \mu_L = 530 \text{ g nm}^{-1} \text{ mol}$$

The value of the persistence length indicates that sPS chains in the molten state are rather rigid as was already observed for iPS in *cis*-decalin<sup>25</sup> and sPS in benzene<sup>17</sup>. The values of the helix radius,  $r_H = 0.62 \pm 0.1$  nm and of the linear mass  $\mu_L = 530 \pm 53 \text{ g nm}^{-1} \text{ mol}$  are consistent with a  $2_1$  helical form for which one expects  $\mu_L = 600 \text{ g nm}^{-1} \text{ mol}$  for deuterated chains and  $r_H = 0.62$  nm. This therefore suggests that the chains take on a near- $2_1$  form in the molten state.

Again, as was found with iPS/*cis*-decalin and sPS/benzene gels, the chains are rigid above the gel melting point. As was already suggested for these systems, the helical form is liable to be stabilized by intercalation of the solvent molecules between the phenyl groups of the chains. Indeed, as can be seen in *Figure 10*, the cavity created by sPS under the  $2_1$  form can house a toluene molecule. This can be expressed in another way: the sPS chains take on the helical form that minimizes the free energy of the polymer-solvent system<sup>27</sup>. This means in particular that the solvent need not be trapped between the phenyl groups. Solvent molecules can exchange, but as long as an outgoing molecule is immediately replaced by an incoming molecule all happens as if the solvent were permanently housed between the phenyl groups. While this model may prove to be efficient for stabilizing the helical form, the exact placement of toluene molecules remains a thorny problem. Detailed calculation of the diffraction structure factors are in progress in an attempt to settle this issue.

If the helical form is stabilized, therefore enhancing chain rigidity, it has been suggested for iPS/*cis*-decalin and sPS/benzene systems that the chains are unable to fold on cooling so that fibres as opposed to spherulites are formed<sup>27</sup>. To be as efficient as possible, stabilization requires one solvent molecule per monomer unit for a  $2_1$

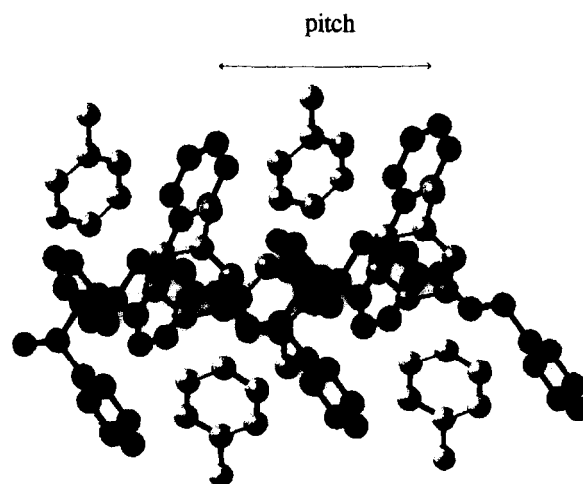


**Figure 10** Possible location of a toluene molecules within the cavities created by phenyl rings as seen parallel to the  $c$ -axis when the chain takes on a  $2_1$  helical form. The actual orientation and position of the toluene molecules with respect to the phenyl rings of the chain are just for illustration purposes. Recent results obtained with benzene<sup>26</sup> suggest parallelism, which could also be the case here

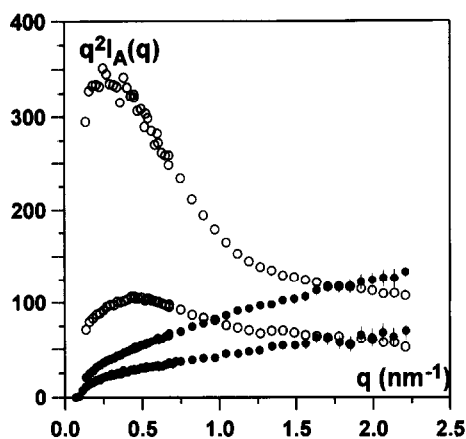


**Figure 11** Neutron scattering curves represented by means of a Kratky plot [ $q^2 I(q)$  versus  $q$ ] for sPS/toluene gel ( $C_p = 0.12$  w/w). Data obtained at two sample–detector distances. Top:  $C_D = 0.06$  (w/w); bottom:  $C_D = 0.03$  (w/w). Full circles stand for the molten state and open circles for the gel state

helix, which corresponds to a 1/1 ‘stoichiometry’. The phase diagrams indicate that this is complied with for the gel state in benzene and chloroform, but not in toluene. Admittedly, the ‘stoichiometry’ may be fulfilled in the molten state, but modified when chain organization takes place at low temperature possibly because the crystalline lattice cannot accommodate totally the 1/1 solvated form; molecular rearrangements may be necessary. At any rate, the fact that the stoichiometry in toluene is lower than one toluene/monomer may explain why rapid cooling rates give the gel while slow cooling rates produce spherulites. Here, kinetics governs the gelation propensity unlike what happens in benzene and chloroform.

The neutron scattering investigations into the gel state do not provide clear-cut results on the chain conformation so that it cannot be decided whether the chains are extended or folded, and therefore confirm that the gel state is produced because chain-folding is impeded. As can be seen in *Figure 11* strong interchain interferences occur in the low  $q$  range that alter the ‘single’ chain signal. This interchain scattering is not due to isotopic segregation, but from the fact that the gelation leads to a phase separation thus concentrating the labelled chains into the fibres. One has to keep in mind that the ratio deuterated chains/hydrogenated chains (sPSD/sPSH ratio) is 1/4 to 1/2 so that if the chains are highly parallel to one another in the fibres, which is a likely situation, a strong interscattering term will dominate the scattered intensity<sup>28</sup>. Only samples where the labelled chains are very diluted are liable not to display this interscattering effect, but then the signal/noise ratio would be too small, particularly at this global polymer concentration of  $C_p = 0.12$  (w/w). Attempts were made to prepare samples with a higher sPS global concentration  $C_p = 0.5$  (w/w) so as to diminish the sPSD/sPSH ratio. They failed because preparing such high concentrations in 1 mm thick quartz cells proved to be exceedingly difficult, particularly for obtaining homogeneous solutions prior to gelation.

There is, however, an interesting outcome from these results: the scattered intensities are the same at large  $q$

values for the gel state and for the molten state. As in this  $q$  range the intensity is only sensitive to the short-range structure, and as it is known from the i.r. spectra that the chains in the gel state take on a  $2_1$  helix, so do the chains in the molten state, thus confirming the above analysis.

## CONCLUDING REMARKS

The phase diagrams established by the investigation into the thermal behaviour of sPS/toluene gels and sPS/chloroform gels show clearly the occurrence of polymer–solvent compounds in both systems. Infra-red spectroscopy investigations, together with neutron scattering and diffraction studies, suggest that the chains are stabilized by toluene intercalation between the phenyl group when the chain is under a  $2_1$  helical form. The same model may hold for chloroform whose molecular size is approximately the same as benzene’s for which this intercalated structure was originally proposed with sPS. As has been stated throughout the paper, structure factor calculations are in progress in an attempt to settle this issue.

## REFERENCES

1. Ishihara, N., Seimija, T., Kuramoto, N. and Uoi, M., *Macromolecules*, 1986, **19**, 2464.
2. Grassi, A., Pellecchia, C., Longo, P. and Zambelli, A., *Gazz. Chim. Ital.*, 1987, **117**, 249.
3. Immirzi, A., De Candia, F., Iannelli, P., Vittoria, V. and Zambelli, A., *Makro. Mol. Chem. Rapid Commun.*, 1988, **9**, 761.
4. Vittoria, V., De Candia, F., Iannelli, P. and Immirzi, A., *Makro. Mol. Chem. Rapid Commun.*, 1988, **9**, 765.
5. Guerra, G., Vitagliano, V. M., De Rosa, C., Petraccone, V. and Corradini, P., *Macromolecules*, 1990, **23**, 1539.
6. De Rosa, C., Guerra, G., Petraccone, V. and Corradini, P., *Polymer*, 1991, **32**, 1435.
7. De Rosa, C., Rapacciuolo, M., Guerra, G., Petraccone, V. and Corradini, P., *Polymer*, 1992, **33**, 1423.
8. Chatani, Y., Shimane, Y., Inagaki, T., Ijitsu, T., Yukinari, T. and Shikuma, H., *Polymer*, 1993, **34**, 1620.
9. Kobayashi, M., Nakaoki, T. and Ishihara, N., *Macromolecules*, 1990, **23**, 78.
10. Daniel, C., Dammer, C. and Guenet, J. M., *Polym. Commun.*, 1994, **35**, 4243.
11. Daniel, C., Deluca, M. D., Brulet, A., Menelle, A. and Guenet, J. M., *Polymer*, 1996, **37**, 1273.
12. Guenet, J. M., *Macromolecules*, 1986, **19**, 1961.
13. Klein, M. and Guenet, J. M., *Macromolecules*, 1989, **22**, 3716.
14. Cotton, J. P., in *Neutron, X-ray and Light Scattering*, ed. P. Lindner and T. Zemb. Elsevier, Paris, 1991.
15. Guenet, J. M. and McKenna, G. B., *Macromolecules*, 1988, **21**, 1752.
16. Kobayashi, M., Nakaoki, T. and Ishihara, N., *Macromolecules*, 1989, **22**, 4377.
17. Vittoria, V., *Polym. Commun.*, 1990, **31**, 263.
18. Vittoria, V., Ruvolo Filho, A. and De Candia, F., *Polym. Bull.*, 1991, **25**, 445.
19. Kobayashi, M. and Kozasa, T., *Appl. Spectrosc.*, 1993, **47**, 1417.
20. Klein, M., Mathis, A., Menelle, A. and Guenet, J. M., *Macromolecules*, 1990, **23**, 4591.
21. Heine, S., Kratky, O., Porod, G. and Schmitz, J. P., *Makromol. Chem.*, 1961, **44**, 682.
22. Des, Cloizeaux, J., *Macromolecules*, 1973, **6**, 403.
23. Pringle, O. A. and Schmidt, P. W., *J. Appl. Crystallogr.*, 1971, **4**, 290.
24. Yoshisaki, T. and Yamakawa, H., *Macromolecules*, 1980, **13**, 1518.
25. Klein, M., Brulet, A., Boué, F. and Guenet, J. M., *Polymer*, 1991, **32**, 1943.
26. Kobayashi, M., 1996, personal communication.
27. Guenet, J. M., *Trends Polym. Sci.*, 1996, **4**, 6.
28. Oster, G. and Riley, D. P., *Acta Crystallogr.*, 1952, **5**, 272.